Ionic bases for electrophysiological distinctions among epicardial, midmyocardial, and endocardial myocytes from the free wall of the canine left ventricle

DW Liu, GA Gintant and C Antzelevitch

Circ. Res. 1993;72;671-687
Circulation Research is published by the American Heart Association. 7272 Greenville Avenue, Dallas, TX 72514
 Print ISSN: 0009-7330. Online ISSN: 1524-4571

Ionic Bases for Electrophysiological Distinctions Among Epicardial, Midmyocardial, and Endocardial Myocytes From the Free Wall of the Canine Left Ventricle

Da-Wei Liu, Gary A. Gintant, and Charles Antzelevitch

Recent studies from our laboratory involving syncytial preparations have delineated electrophysiological distinctions between epicardium, endocardium, and a unique population of cells in the deep subepicardial to midmyocardial layers (M region) of the canine ventricle. In the present study, we used standard microelectrode, single microelectrode switch voltage-clamp, and whole-cell patch-clamp techniques to examine transmembrane action potentials, steady-state current–voltage relations, and the 4-aminopyridine–sensitive transient outward current (I_{to1}) in myocytes enzymatically dissociated from discrete layers of the free wall of the canine left ventricle. Action potential characteristics of myocytes isolated from the epicardium, M region, and endocardium were very similar to those previously observed in syncytial preparations isolated from the respective regions of the ventricular wall. A prominent spike and dome was apparent in myocytes from epicardium and the M region but not in myocytes from endocardium. Action potential duration–rate relations were considerably more pronounced in cells isolated from the M region. Current–voltage relations recorded from cells of epicardial, M region, and endocardial origin all displayed an N-shaped configuration with a prominent negative slope–conductance region. The magnitude of the inward rectifier K^+ current (I_{K1}) was 392±86, 289±65, and 348±115 pA in epicardial, M region, and endocardial myocytes, respectively, when defined as steady-state current blocked by 10 mM Cs^+. Similar levels were obtained when I_{K1} was defined as the steady-state difference current measured in the presence (6 mM) and absence of extracellular K^+. I_{to1} was significantly greater in epicardial and M region myocytes than in endocardial myocytes. At a test potential of +70 mV (holding potential, −80 mV), I_{to1} amplitude was 4,203±2,370, 3,638±1,135, and 714±286 pA in epicardial, M region, and endocardial cells, respectively. No significant differences were observed in the voltage dependence of inactivation of I_{to1} in the three cell types. The time course of reactivation of I_{to1} was slower in cells from the M region compared with either epicardial or endocardial cells. Our data suggest that prominent heterogeneity exists in the electrophysiology of cells spanning the canine ventricular wall and that differences in the intensity of the transient outward current contribute importantly, but not exclusively, to this heterogeneity. These findings should advance our understanding of basic heart function and the ionic bases for the electrocardiographic J wave, T wave, U wave, and long QT intervals as well as improve our understanding of some of the complex factors contributing to the development of cardiac arrhythmias. (*Circulation Research* 1993;72:671–687)

KEY WORDS • ventricular myocardium • epicardium • endocardium • midmyocardium • M cells • electrophysiology • heterogeneity • ionic currents • transient outward currents • inward rectifier currents

Although electrophysiological heterogeneity within the mammalian ventricle has long been recognized, a systematic study of the electrophysiological and pharmacological distinctions between different regions of the heart and the ionic bases for these differences has been lacking (for review see Reference 1). Recent studies from our laboratory have delineated several electrophysiological distinctions between epicardial and endocardial tissues isolated from the canine ventricles.[1–4] Chief among these was the presence of a prominent "spike and dome" action potential morphology in epicardial but not endocardial tissues. This distinction has also been described in the canine heart in vivo[5,6] and in rabbit[7] and feline[8] ventricular myocytes studied in vitro. More recent studies have described a unique subpopulation of cells (M cells) in the deep

From the Masonic Medical Research Laboratory, Utica, N.Y.

Previously presented as preliminary results in abstract form (*PACE* 1992;15[suppl II]:537).

Supported by grant HL-37396 from the National Institutes of Health and grants from the American Heart Association, New York State Affiliate, Inc., the Charles L. Keith and Clara Miller Foundation, and the Josephine Lawrence Hopkins Foundation.

D.-W.L. was awarded first prize in the Young Investigator Award Competition of the North American Society of Pacing and Electrophysiology for this work.

Address for correspondence: Dr. Charles Antzelevitch, Masonic Medical Research Laboratory, 2150 Bleecker Street, Utica, NY 13504.

Received July 16, 1992; accepted December 7, 1992.

subepicardial to midmyocardial layers (M region) of the canine ventricle. M cells were found to display electrophysiological features intermediate between those of myocardial and conducting cells[9] and pharmacological responsiveness different from that of either epicardium or endocardium.[10,11] M cell action potentials display a spike and dome morphology similar to that recorded from epicardium but a maximal rate of rise of the action potential upstroke that is considerably greater than that of either endocardium or epicardium. The hallmark of the M cell is its ability to prolong with deceleration of the stimulation rate. The rate dependence of action potential duration (APD) in the M region is much more accentuated than that of either epicardium or endocardium but more akin to that of Purkinje fibers.

The presence of a prominent transient outward current (I_{to}) in canine ventricular epicardium but not endocardium has been suggested as the basis for the prominent spike and dome morphology of the epicardial action potential, which is greatly diminished or lacking in endocardium.[4] Although this hypothesis has not yet been tested in canine ventricular myocytes, recent voltage-clamp studies using myocytes isolated from the ventricular epicardium and endocardium of cat and rabbit hearts have reported regional differences in the intensity of the I_{to} consistent with the hypothesis.[7,12]

The present study was designed with two major goals in mind: 1) to characterize the electrophysiological features of myocytes isolated from the epicardium, M region, and endocardium of the canine left ventricular free wall and thus assess to what extent the electrophysiological distinctions observed in the syncytial preparations are maintained in myocytes enzymatically dissociated from the respective regions of the canine ventricle and 2) to examine the ionic bases for the electrophysiological distinctions among these three cell types, focusing on I_{to} and the inward rectifier K^+ current (I_{K1}).

Materials and Methods

Isolation of Cardiac Myocytes

Isolated myocytes were prepared in a manner similar to that described by Hewett et al.[13] Briefly, adult mongrel dogs of either sex were anesthetized with sodium pentobarbital (30 mg/kg i.v.), and their hearts were quickly removed and placed in normal Tyrode's solution. A wedge consisting of that part of the left ventricular free wall supplied by the left anterior descending coronary artery was excised. The left anterior coronary artery was cannulated and flushed with Ca^{2+}-free "Krebs' buffer" (mM: NaCl 118.5, KCl 2.8, $NaHCO_3$ 14.5, KH_2PO_4 1.2, $MgSO_4$ 1.2, and glucose 11.1) supplemented with 0.1% bovine serum albumin (BSA, fraction V, Sigma Chemical Co., St. Louis, Mo.) and gassed with 95%O_2–5%CO_2 for 3 minutes at a rate of 12 ml/min. Perfusion was then switched to 75 ml Ca^{2+}-free Krebs' buffer containing 75 mg BSA and 37.5 mg collagenase (CLS 2, 171 units/mg, Worthington Biochemical Corp., Freehold, N.J.) for 20–30 minutes at 37°C (95%O_2–5%CO_2, with recirculation). After perfusion, thin slices of tissues were dissected from epicardium (<2 mm from the epicardial surface), M region (2–7 mm from the epicardial surface), and endocardium (<2 mm from the endocardial surface) using fine scissors or a dermatome (Davol Simon Dermatome power handle No. 3293 with cutting head No. 3295). Shavings were made parallel to the surface of the left ventricular free wall midway along the apicobasal axis. Tissues from each region were placed into separate beakers, minced, incubated in fresh Krebs' buffer containing 0.5 mg/ml collagenase, 3% BSA, and 0.3 mM $CaCl_2$, and agitated with 95%O_2–5%CO_2. Incubation was repeated three to five times at 15-minute intervals with fresh enzyme solution. The supernatant from each digestion was filtered (220-μm mesh) and centrifuged (200–300 rpm for 2 minutes). Cells were then stored in a HEPES-buffered Tyrode's solution (see below) supplemented with 0.5 mM Ca^{2+} at room temperature for later use.

To more precisely identify the origin of cells, in some cases, we used the "chunk" method for cell dissociation (modified from Barrington et al[14]). Thin slices (0.5–1.0 mm) of epicardial, deep subepicardial (M region), and endocardial tissues (as previously defined) were shaved from the left ventricular free wall midway along the apicobasal axis by use of a dermatome. The tissues were rinsed with normal Tyrode's solution and cut into pieces of approximately 1×1 cm^2. Four to eight pieces of tissues were placed in Ca^{2+}-free trituration solution (mM: NaCl 135, KCl 5, $MgSO_4$ 1, D-glucose 10, and HEPES 10, pH 7.4, bubbled with 100% O_2) supplemented with collagenase (0.5 mg/ml) and BSA (1%) and stirred with a magnetic bar at room temperature. The incubation solution was replaced five or six times at 30-minute intervals. After the first three digests, the supernatant was collected after each digest and centrifuged at 400 rpm. The cell pellet was then resuspended in a HEPES-buffered Tyrode's solution (see below) containing 0.5 mM Ca^{2+}.

Electrophysiology

An aliquot of cells was placed on a poly-L-lysine–coated coverslip in a temperature-controlled superfusion bath (Medical Systems Corp., Greenvale, N.Y.) mounted on the stage of an inverted microscope (Nikon Diaphot, Nikon Instruments, Japan). Cells were allowed to adhere to the coverslip for 5 minutes and were then continuously superfused with a HEPES-buffered Tyrode's solution at a flow rate of 2 ml/min. The typical superfusate composition was (mM) NaCl 132, KCl 6, $CaCl_2$ 2, $MgSO_4$ 1.2, HEPES 20, and glucose 11.1, pH-adjusted with NaOH to 7.35 and aerated with 100% O_2. Only relaxed quiescent cells displaying prominent cross striations were used. All experiments were performed at 35–37°C; temperature was maintained constant within 0.5°C during any given experiment.

To minimize alterations of the intracellular milieu, action potential studies were performed using standard microelectrode techniques. Transmembrane action potentials were recorded from individual myocytes by use of microelectrodes filled with 2.7 M KCl (resistance, 20–50 MΩ) and an Axoclamp-2A amplifier with an HS-2L gain ×0.1 head stage (Axon Instruments, Foster City, Calif.) in bridge mode. The bath was grounded through a KCl Ag/AgCl salt bridge. Cells were stimulated by injection of current pulses of 1–2-msec duration at basic cycle lengths ranging between 300 and 8,000 msec.

Steady-state current–voltage (I-V) relations were determined using a single microelectrode discontinuous

voltage-clamp technique. Slow depolarizing ramps (approximately 8–12 mV/sec) from approximately −90 mV to 0 (or +10) mV were applied. A switching frequency of 2–8 kHz was used. The voltage signal before the sample hold unit was monitored continuously to ensure that voltage drop across the tip resistance subsided completely between current injection cycles. In another series of experiments, steady-state I-V relations were determined using the whole-cell patch-clamp technique. Two-second hyperpolarizing and depolarizing voltage steps were applied from a holding potential of −50 mV. Tetrodotoxin (TTX, 15–30 μM), $MnCl_2$ (2 mM), and ouabain (2–5 μM) were used throughout the course of these experiments to block the sodium, calcium, and Na^+-K^+ pump currents, respectively.

I_{to} was measured using standard whole-cell patch-clamp techniques.[15] An Axopatch-1D amplifier with a CV-4 1/100 head stage (Axon Instruments) was used in these studies. Suction pipettes made of borosilicate glass (1.5 mm o.d. and 1.1 mm i.d., Becton, Dickinson and Co., Parsippany, N.J.) were pulled on a Flaming-Brown–type pipette puller (Sutter Instrument Co., Novato, Calif.) and fire-polished before use. Pipette tip resistances measured in Tyrode's solution were 2–3 MΩ when filled with internal solution containing (mM) potassium aspartate 125, KCl 20, $MgCl_2$ 1, ATP (Mg salt) 5, HEPES 5, and EGTA 10. The pH of the pipette solution was adjusted to 7.3 with KOH, and the solution was passed through a sterile 0.22-μm filter (Millipore Corp., Bedford, Mass.) before use. The junction potential between the pipette solution and Tyrode's solution was zeroed before formation of the membrane–pipette seal in normal Tyrode's solution (15 mV; see Reference 16). This zeroing created an offset equal to the junction potential, but of opposite sign, that remained after the establishment of whole-cell recording. All voltages in the patch-clamp experiments were corrected for this offset. Once the suction pipette made a gigaohm seal with the cell, the pipette capacitance was neutralized. The membrane was ruptured by applying additional negative pressure. Cell capacitance and series resistance were partially compensated electronically in some experiments. Currents recorded using whole-cell patch techniques were obtained at least 10 minutes after cell break-in to allow for equilibration of the intracellular space with the pipette solution.

Data Acquisition and Analysis

An Everex 386 computer equipped with 12-bit AD/DA converters (model 1401, Cambridge Electronic Design, Cambridge, England) was used for data acquisition and generation of pulse template and command potentials for both current and voltage-clamp modes (VCLAMP software module). Currents were filtered with a four-pole Bessel filter at 5 kHz and digitized at 10 kHz.

To analyze the voltage-dependent 4-aminopyridine (4-AP)–sensitive component of the transient outward current (I_{to1}), it is necessary to minimize other temporally superimposed currents. L-type calcium current (I_{Ca}) was blocked using 2 mM manganese in the external solution.[16] T-type I_{Ca}, thought to be relatively small in canine ventricular myocytes, is also reduced by manganese.[17] The calcium-activated component of I_{to} (I_{to2}) was suppressed by block of I_{Ca} using external manganese and/or use of 10 mM EGTA in the pipette solution (pCa was estimated to be 10).[16,18,19] In most experiments, the sodium current (I_{Na}) was partially blocked using 15–30 μM TTX. Under these conditions, the I_{to} obtained was >75% suppressed with 5 mM 4-AP, suggesting that it is predominantly I_{to1}. The amplitude of I_{to1} was measured in this study as the difference between the outward current peak and the maintained current level approximately 150 msec after the onset of the depolarizing pulse.

Cell capacitance was calculated by integrating the area under the uncompensated capacitative transient induced by a 5-mV hyperpolarization step from approximately −40 mV and dividing this area by the voltage step. Accuracy was verified by measurement of the time constant of decay of the capacity transient, which was then divided by the series resistance. The capacitance values for myocytes from epicardium, M region, and endocardium are listed in Table 1. We also measured the maximum widths and lengths as well as surface areas by using photographs of the cells. These data are also included in Table 1. No significant differences could be discerned in the capacitance or physical dimensions of the three different cell types.

TTX (Calbiochem Corp., La Jolla, Calif., or Sigma) was prepared as a 1 mg/5 ml stock solution and added to the Tyrode's solution as required. 4-AP, $MnCl_2$, CsCl, and ouabain (Sigma) were prepared from stock solution just before use. The pH of the Tyrode's solution was monitored after addition of 4-AP and, when necessary, adjusted to 7.35 using HCl.

Curves were fit using nonlinear least-squares regression techniques. Where possible, data are presented as mean±SD. Statistical analysis of the data was performed using analysis of variance coupled with Scheffe's or Tukey's procedure.

Results

Action Potential Characteristics

Figure 1 illustrates transmembrane activity recorded by standard microelectrode technique from epicardial (top tracings), M region (middle tracings), and endocardial (bottom tracings) myocytes stimulated at two different basic cycle lengths (BCLs). At a BCL of 300 msec, the three cell types display fairly similar APDs. The main distinguishing feature is the presence of a notch in action potentials recorded from epicardial and M region myocytes but not in activity recorded from the endocardial cell. This distinction is still more striking at slower stimulation rates. At a BCL of 8,000 msec (Figure 1, right tracings), a prominent spike and dome morphology develops in epicardial and M cell responses, but action potentials recorded from the endocardial cell show little or no notch even at these very slow frequencies. Another important distinction becomes obvious at slow stimulation rates: the action potentials of the M cell prolong disproportionately. Slowing of the stimulation rate from a BCL of 300 to 8,000 msec caused a 282-msec prolongation of APD measured at 90% repolarization (APD_{90}) in myocytes from the M region but a much more modest increase of APD_{90} in epicardial (85 msec) and endocardial (65 msec) myocytes. APD_{90} values at a BCL of 2,000 msec averaged 233±21 (n=13), 252±23 (n=11), and 402±51

TABLE 1. Measurements of Cell Capacitance and Physical Dimensions

	Region		
	Epicardium	Midmyocardium	Endocardium
C_m (pF)			
Mean±SD	150±34	142±27	145±44
n	19	30	16
Surface area (μm^2)			
Mean±SD	4,206±1,264	4,307±767	4,902±628
n	16	26	7
Maximum length (μm)			
Mean±SD	192±28	189±25	196±20
n	16	26	7
Maximum width (μm)			
Mean±SD	30±6	33±4	35±5
n	16	26	7

C_m, membrane capacitance; *n*, number of cells studied.
Surface area values represent two-dimensional areas of the outline of cells measured from photographs of the magnified images.

(n=12) msec in myocytes from epicardium, endocardium, and M region, respectively.

Rate Dependence Under Steady-State Conditions

Rate-dependent changes in action potential characteristics of myocytes isolated from epicardium, M region, and endocardium of the left ventricular free wall are compared with those of syncytial tissues isolated from these regions in Figures 2 and 3. Standard microelectrode techniques were used to record transmembrane activity from tissue preparations as well as myocytes. The BCL was varied from 300 to 5,000 or 8,000 msec, and data were collected after achievement of a steady state. Each panel in Figure 2 comprises four or five superimposed tracings representing action potentials recorded at the different BCLs. The results obtained in tissues are from a recent study by Sicouri and Antzelevitch.[9]

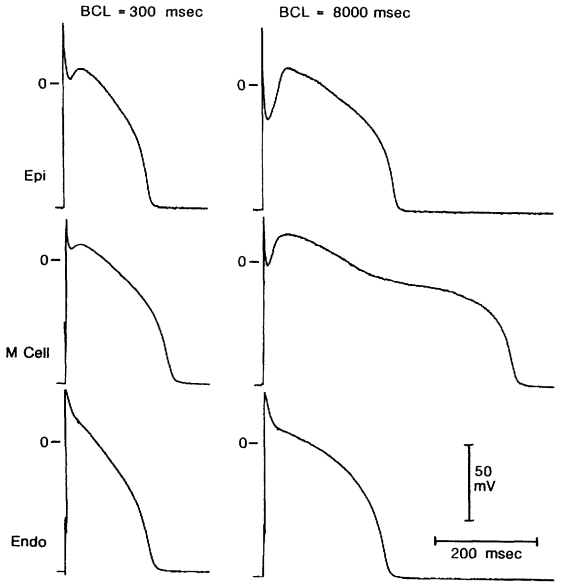

FIGURE 1. *Transmembrane action potentials recorded from myocytes isolated from the epicardial (Epi), midmyocardial (M cell), and endocardial (Endo) regions of the canine left ventricular free wall. Action potential recordings were obtained using standard microelectrodes at stimulation basic cycle lengths (BCLs) of 300 and 8,000 msec. Relatively small differences in action potential morphology are evident at a BCL of 300 msec. Slower stimulation rates give rise to a prominent spike and dome morphology in epicardial and M cells and a markedly prolonged action potential in the M cell. $[K^+]_o$ was 6 mM.*

A prominent rate-dependent spike and dome is apparent in the myocytes and tissues of epicardial and midmyocardial (M cell) origin but not in those of endocardial origin. A gradual shift in BCL from 300 to 8,000 msec leads to a progressive accentuation of the spike and dome configuration of the action potential in epicardial tissues and cells (Figure 2, top tracings). Phase 1 becomes more prominent, and the peak plateau is achieved later, usually reaching a more positive potential. Accentuation of the notch is seen to contribute to the overall prolongation of APD_{90} in epicardium. Deceleration-induced accentuation of the spike and dome morphology of the action potential is also observed in the M cell preparations. The overall contribution of the changes in phase 1 to rate dependence of APD, however, appears less important than in epicardium. In both tissues and cells from the M region, deceleration was attended by a progressive and remarkable prolongation of the action potential principally because of progressive delays in the onset of final repolarization. In contrast to the marked changes in phase 1 of epicardial and M cell activity, little or no rate-dependent changes are observed in the early phases of the endocardial action potential. Qualitatively similar results were obtained in 45 experiments involving myocytes. In all cases, the congruity between the myocyte and tissue data was exceptional. Similar behavior was observed despite the fact that the myocytes were superfused with Tyrode's solution containing 6 mM $[K^+]_o$, whereas the tissue studies were performed using Tyrode's containing 4 mM $[K^+]_o$.

The rate dependence values of APD_{90} for the cell and tissue preparations pictured in Figure 2 are graphically

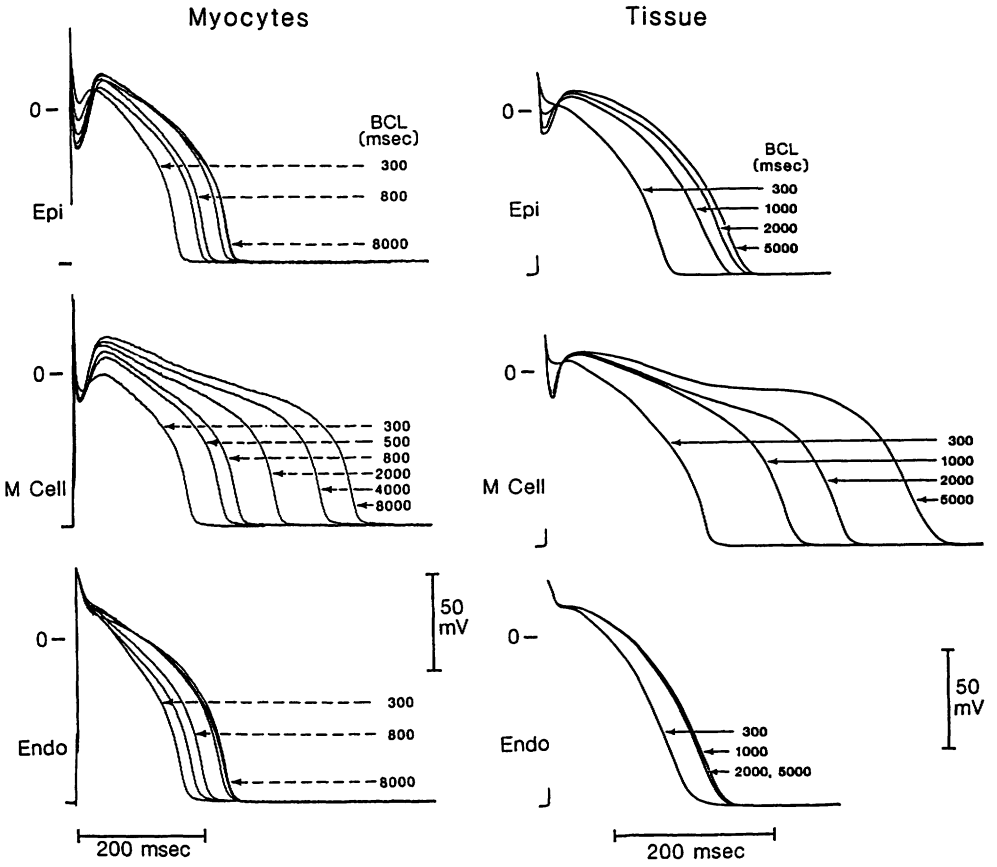

FIGURE 2. *Comparison of the electrophysiological characteristics of myocytes (left panel) and syncytial preparations (right panel) isolated from epicardial (Epi), midmyocardial (M cell), and endocardial (Endo) regions of the canine left ventricular free wall. Each panel shows superimposed action potentials recorded at basic cycle lengths (BCLs) of 300 to 5,000 or 8,000 msec. All action potentials were recorded using standard microelectrode techniques. Tissue results are from Reference 9. Note that the extracellular potassium concentration was 6 mM for myocytes and 4 mM for tissues.*

illustrated in Figure 3. At a BCL of 300 msec, all three cell and tissue types display relatively brief action potentials of similar duration; at a BCL of 8,000 msec, the M cell response prolongs to nearly twice the duration seen in the endocardial or epicardial myocytes. A much steeper APD–rate relation is observed in myocytes from the M region, and once again the myocyte data are congruent with data obtained from syncytial tissue preparations (Figure 3).

The marked accentuation of the spike and dome configuration in canine ventricular epicardial and M cells with deceleration is thought to be due to a prominent contribution of a slowly reactivating I_{to} to the electrical response of these cells.[4] The slow kinetics of recovery of the current are believed to be directly responsible for the slow restitution of the notch or spike and dome configuration of the action potential. These characteristics of ventricular myocytes are illustrated in Figure 4.

Restitution of Action Potential Parameters in Ventricular Myocytes

The first response in each panel of Figure 4 is the last of a train of 10 beats elicited with stimulus (S_1) applied at a BCL of 2,000 msec. Subsequent beats are responses to premature beats introduced at progressively longer S_1–S_2 intervals. Restitution of action potential parameters is thus illustrated in myocytes of epicardial, M region, and endocardial origin. In M region and epicardial myocytes, the spike and dome morphology of the action potential is absent in early premature beats and is seen to gradually recover in less premature responses. These time-dependent changes in the early phases of the action potential are not observed in endocardial myocytes.

Ionic Currents

The ionic basis for the electrophysiological distinctions between cells and tissues of epicardial, M region, and endocardial origin is the subject of intensive investigation at our laboratory as well as others. In this study, we report on differences and similarities in I_{K1} and I_{to} in the three predominant cell types.

Steady-State Current–Voltage Relation and Inward Rectifier Potassium Current

Steady-state I-V relations were examined in epicardial, M region, and endocardial myocytes by application of a slowly depolarizing voltage ramp (8–10 mV/sec) from approximately −90 mV to 0 or +10 mV by using the single microelectrode switch voltage-clamp technique. The representative results illustrated in Figure 5A show that all three cell types display a similar N-shaped I-V configuration with a prominent negative

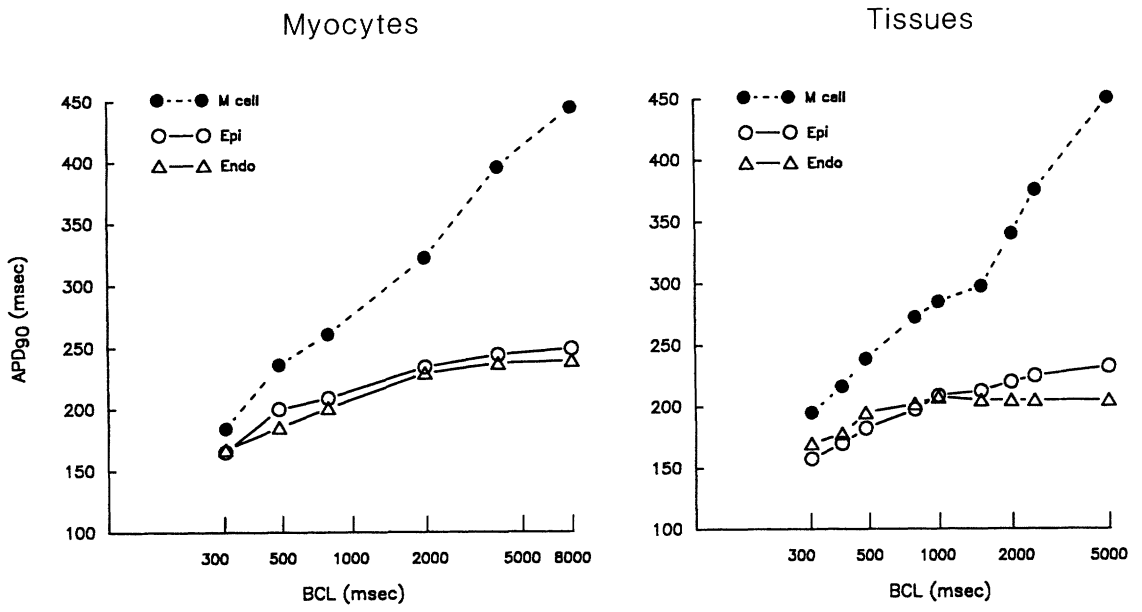

FIGURE 3. *Graph showing action potential duration (APD)–rate relations for myocytes (left panel) and syncytial preparations (right panel) isolated from epicardial (Epi), midmyocardial (M cell), and endocardial (Endo) regions of the canine left ventricular free wall. BCL, basic cycle length. APD values are those of responses pictured in Figure 2 measured at 90% repolarization (APD_{90}). A much steeper APD–rate relation is observed in myocytes and tissues from the M region as compared with epicardium or endocardium. Tissue results are from Reference 9.*

slope conductance region. I_{K1} was measured as the current blocked by 10 mM CsCl. I-V relations denoted by the filled squares were recorded after the addition of Cs^+ to the superfusate. I_{K1}, defined as the Cs^+-sensitive component, was obtained by subtracting currents before and after CsCl (Figure 5B). We could not discern any major differences in the configuration and magnitude of I_{K1} in the three cell types. The average peak magnitudes of I_{K1} were 392±86 pA (n=6) for epicardial, 289±65 pA (n=7) for M region, and 348±115 pA (n=8) for endocardial myocytes.

To exclude the possibility that the different cell types may have different sensitivities to Cs^+, we performed another series of experiments in which time-independent currents were measured in the presence and absence of extracellular K^+ by the whole-cell patch-clamp technique. TTX (15 μM), $MnCl_2$ (2 mM), and ouabain (2–5 μM) were used throughout the experiment to block sodium, calcium, and Na^+-K^+ pump currents, respectively. Figure 6 shows the voltage protocol used and the representative current recordings obtained under these conditions. Steady-state I-V relations were constructed by plotting the current levels at the end of 2-second pulses from a holding potential of −50 mV to test potentials ranging between −100 and +30 mV (Figure 6B). I_{K1} was isolated by subtracting the currents recorded in the presence (6 mM) and absence of extracellular potassium. Composite data of I-V and current density–voltage relations of I_{K1}, measured under these conditions, are illustrated in Figure 7. Our results indicate that I_{K1} isolated in this manner is similar to that measured as Cs^+-sensitive current by using either voltage-step or ramp protocols. No significant difference in I_{K1} could be discerned among the three cell types.

Characteristics of the Transient Outward Current in Canine Ventricular Myocytes

The action potential data thus far presented, coupled with data from previous studies involving syncytial tissues, suggest important differences in the contribution of I_{to} to the electrical activity of cells spanning the canine ventricular wall. Using whole-cell patch-clamp techniques, we set out to systematically characterize I_{to} in epicardial, M region, and endocardial myocytes. Figure 8 illustrates the results of a representative experiment. The action potentials shown in the left panel were recorded using a patch pipette under the whole-cell current-clamp mode (BCL, 2,000 msec). Figure 8A serves to illustrate that the salient features of transmembrane activity of the three distinct cell types are maintained under these recording conditions. Thus, in this experiment and several others in which ionic currents were evaluated, we were able to distinguish between M cells, epicardial cells, and endocardial cells not only on the basis of their anatomic source (level of the ventricular wall from which they were isolated) but also on the basis of their action potential characteristics.

To assess the contribution of I_{to} in these cells, we clamped the membrane potential for 300 msec to a test potential between −40 and +70 mV in 10-mV steps from a holding potential of −80 mV. Figure 8B shows membrane currents recorded in response to test pulses ranging between +30 and +70 mV. The current tracing shows a time-dependent I_{to} with rapid activation and inactivation kinetics. I_{to} was most prominent in the epicardial myocyte, somewhat less prominent in the M cell, and smallest in the endocardial cell. The I_{to} recorded under these conditions was largely abolished by exposure of the myocytes to 5 mM 4-AP (data not shown), suggesting that it is the predominantly 4-AP–

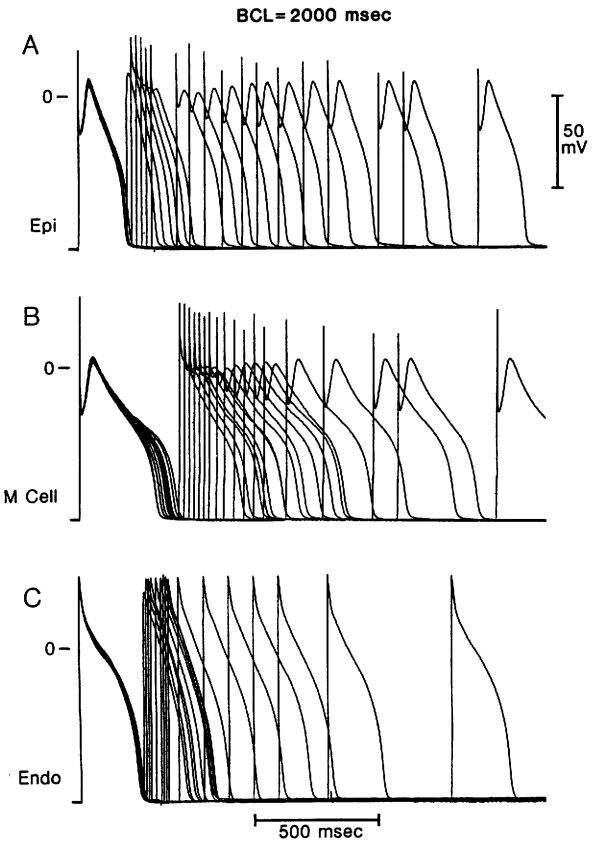

FIGURE 4. *Tracings showing restitution of action potential parameters in myocytes from epicardial (Epi, panel A), midmyocardial (M cell, panel B), and endocardial (Endo, panel C) regions. The first response in each panel is the last of a train of 10 basic beats. Subsequent beats represent responses to premature stimuli introduced progressively later in the cycle. The spike and dome morphology recovers slowly in Epi and M cell regions. The Endo cell shows little, if any, time-dependent changes in the early phases of the action potential. Note that some of the phase 0 amplitudes are not accurate because of the relatively slow sampling rate used in these recordings. Basic cycle length (BCL) was 2,000 msec.*

sensitive component of I_{to}, commonly referred to as I_{to1}. The calcium-activated component, frequently referred to as I_{to2}, is largely eliminated by the calcium buffering of the internal pipette solution with 10 mM EGTA. The voltage dependence of peak current measured in 14 cells is graphically summarized in Figure 9. At a test voltage of +70 mV, the mean amplitude of I_{to1} was 4,551±1,740 pA in epicardial myocytes, 3,700±1,006 pA in M cells, and 577±79 pA in endocardial cells. All epicardial and M cell measurements of I_{to1} positive to a test potential of +10 mV were significantly different from the current levels measured in endocardial cells. Differences between epicardial and M cells were not statistically significant at any potential.

The results presented in Figures 8 and 9 are from experiments in which no attempt was made to block any other current. This enabled us to record the action potential and ionic currents within several minutes of each other and thus to gauge as directly as possible the influence of I_{to} magnitudes on action potential morphology. Because activation of I_{to} overlaps that of I_{Na} and I_{Ca}, in another experimental series we blocked these inward currents using TTX (15–30 μM) and $MnCl_2$ (Mn^{2+}, 2 mM). Most experiments involving characterization of the voltage dependence of activation and inactivation as well as the kinetics of reactivation were performed in the presence of these inward current blockers.

Figure 10 shows the results obtained when the protocols described for Figures 8 and 9 were repeated in cells pretreated with TTX and Mn^{2+}. It is noteworthy that little if any difference was apparent in the voltage dependence of peak current in the presence and absence of Mn^{2+} and TTX (compare with Figures 9 and 10B). Very large and fast transient outward currents were consistently recorded from epicardial and M region myocytes. In contrast, I_{to1} recorded from endocardial myocytes was always very small (Figure 10). All epicardial and M cell measurements of I_{to1} positive to a test potential of 0 mV were significantly different from the current levels measured in endocardial cells. Once again, we found no statistical significance between peak I_{to1} measured in epicardial and M cells. At a test voltage of +70 mV, the mean amplitude of I_{to1} was 4,203±2,370 pA in epicardial myocytes (n=7), 3,638±1,135 pA in M cells (n=14), and 714±286 pA in endocardial cells (n=7). It should be noted that M cells used to collect data for Figure 9 were isolated from the entire M region (deep subepicardium to midmyocardium), whereas those used to generate data for Figure 10 were principally from the deep subepicardium. The reason for limiting our tissue source for M cells in the patch-clamp experiments stems from the fact that action potential experiments using standard microelectrodes in myocytes (as well as tissues) indicated that the cells with the most pronounced M cell behavior (steep APD–rate relation) were found in the deep subepicardium. As will be discussed later, a variety of transitional cell types are also encountered in the M region, but less so in the deep subepicardium.

The regional differences in the amplitude of I_{to} could be caused by a number of factors. One possibility is that measured differences in outward current may in fact reflect differences in inward currents such as I_{Na} and I_{Ca} (T and L type), whose activation overlaps that of I_{to}. Although the experiments illustrated in Figure 10 were conducted in the presence of 2 mM Mn^{2+} and 15–30 μM TTX, an inward current is readily apparent in the endocardial recordings. Since 2 mM Mn^{2+} blocks most I_{Ca} in canine ventricular myocytes,[16,17] the inward current apparent in our endocardial recordings is likely due to incomplete TTX block of I_{Na}. It is possible that this residual inward current may cause an underestimation of the peak I_{to}, particularly at modest test voltages; however, this influence should dissipate at more positive test potentials, approaching the reversal potential for I_{Na} (and I_{Ca}). The persistence of differences in outward current at +70 mV argues against a major contribution of inward currents to the measured differences in I_{to}.

Another possible explanation for the regional differences in I_{to} is that the threshold for activation of I_{to} is shifted to more positive potentials in endocardial versus epicardial and M region myocytes. This does not seem likely, since the peak I-V relations do not appear shifted along the voltage axis but are simply scaled down. Thus, the normalized peak I-V relations are almost superim-

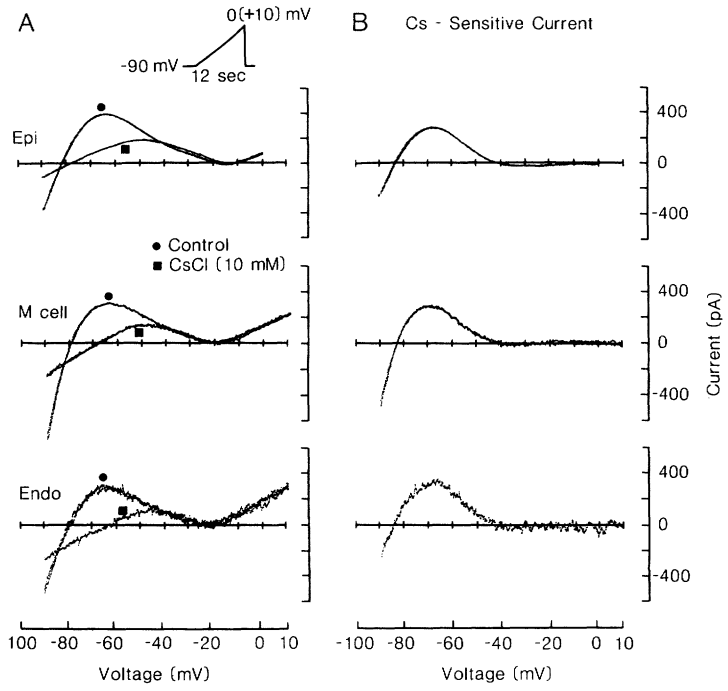

FIGURE 5. *Representative steady-state current–voltage relations and inward rectifier current in three ventricular cell types. Panel A: Recordings of steady-state current–voltage relations for myocytes of epicardial (Epi), midmyocardial (M cell), and endocardial (Endo) origin. Current–voltage curves were obtained under control conditions (Tyrode's solution, filled circles) and after the addition of 10 mM CsCl (filled squares) using slowly depolarizing ramp clamps (8–10 mV/sec). All three cell types display regions of inward rectification, negative slope, and outward rectification. Panel B: The inward rectifier K^+ current (I_{KI}) in the three cell types, obtained by subtraction of currents recorded before and after Cs^+ (Cs^+-sensitive component). No significant differences were discerned in the configuration or amplitude of I_{KI} among the three different cell types. $[K^+]_o$ was 6 mM; recordings were obtained using single microelectrode switch voltage-clamp technique.*

posable (Figure 11). Another possibility is that the voltage dependence of inactivation of I_{to1} is different, resulting in different levels of steady-state inactivation of the current at the same resting potential.

Voltage Dependence of Inactivation of the Transient Outward Current

The voltage dependence of inactivation of I_{to1} was studied by clamping the cell at various preconditioning voltages (V_c) for 1 second from a holding potential of −80 mV and then to a test potential of +40 mV. The interval between test pulses was 10 seconds. Normalized inactivation curves recorded from representative cells of epicardial, M region, and endocardial origin are illustrated in Figure 12. The peak amplitude of I_{to1} during the test pulse was normalized to the maximum amplitude of current recorded in each group. The inactivation curves of the three cell types were virtually superimposable and thus were fit as a group to a Boltzmann distribution function:

$$\text{Inactivation variable} = \{1+\exp[(V_c - V_{0.5})/k]\}^{-1}$$

where $V_{0.5}$ is the half-maximal inactivation voltage (−34.9 mV) and k is the slope factor (k=3.6). Similar results were obtained in 11 other experiments; the mean value of $V_{0.5}$ for the entire group was −40±8.3 mV. These data indicate that differences in voltage dependence of inactivation cannot explain the regional differences in I_{to1} amplitude. Another possibility is that the kinetics of reactivation, especially near the resting potential, are different in the different cell types.

Transient Outward Current Reactivation Kinetics

We examined the time course of recovery of I_{to1} from inactivation (reactivation) using a standard double-pulse protocol. Twin voltage pulses (from −80 to +40 mV, 200-msec duration) were applied once every 10 seconds with varying interpulse intervals. Figure 13 shows the results of an experiment performed using a cell from the M region of the left ventricular free wall. The I_{to1} amplitude of the second pulse is plotted as a fraction of the I_{to1} amplitude of the first. The current was nearly absent with an interpulse interval of 10 msec and increased gradually at longer intervals. The reactivation time course was well fit with a biexponential process with fast and slow time constants (40 and 270 msec, respectively; see Figure 13 inset). Figure 14 presents the results of 15 experiments in which reactivation kinetics were evaluated. Two exponential processes were apparent in all the cells studied. The fast time constant averaged 35±10, 57±35, and 57±10 msec in cells of epicardial, M region, and endocardial origin, respectively. The slow time constant averaged 264±71, 456±212, and 390±61 msec in cells of epicardial, M region, and endocardial origin, respectively. The average values of both slow and fast time constants in M cells were longer than those of epicardial and endocardial cells, but this difference did not achieve statistical significance. Likewise, no significant difference could be discerned between the time course of reactivation of epicardial and endocardial cells.

Discussion

Action Potential Characteristics

Previous studies from our laboratory have defined important electrophysiological and pharmacological distinctions between epicardium, endocardium, and the M region (deep subepicardial to midmyocardial layers) of the canine ventricular free wall.[1–4,9,11,20–23] The extent to which these regional dissimilarities reflect intrinsic properties of the cells has previously not been fully appreciated. Moreover, the ionic bases for many of the electrophysiological distinctions are unknown. These issues are not readily amenable to study in tissue preparations but can be more directly addressed through isolation and evaluation of single cells from distinct layers of the ventricular wall. In the present

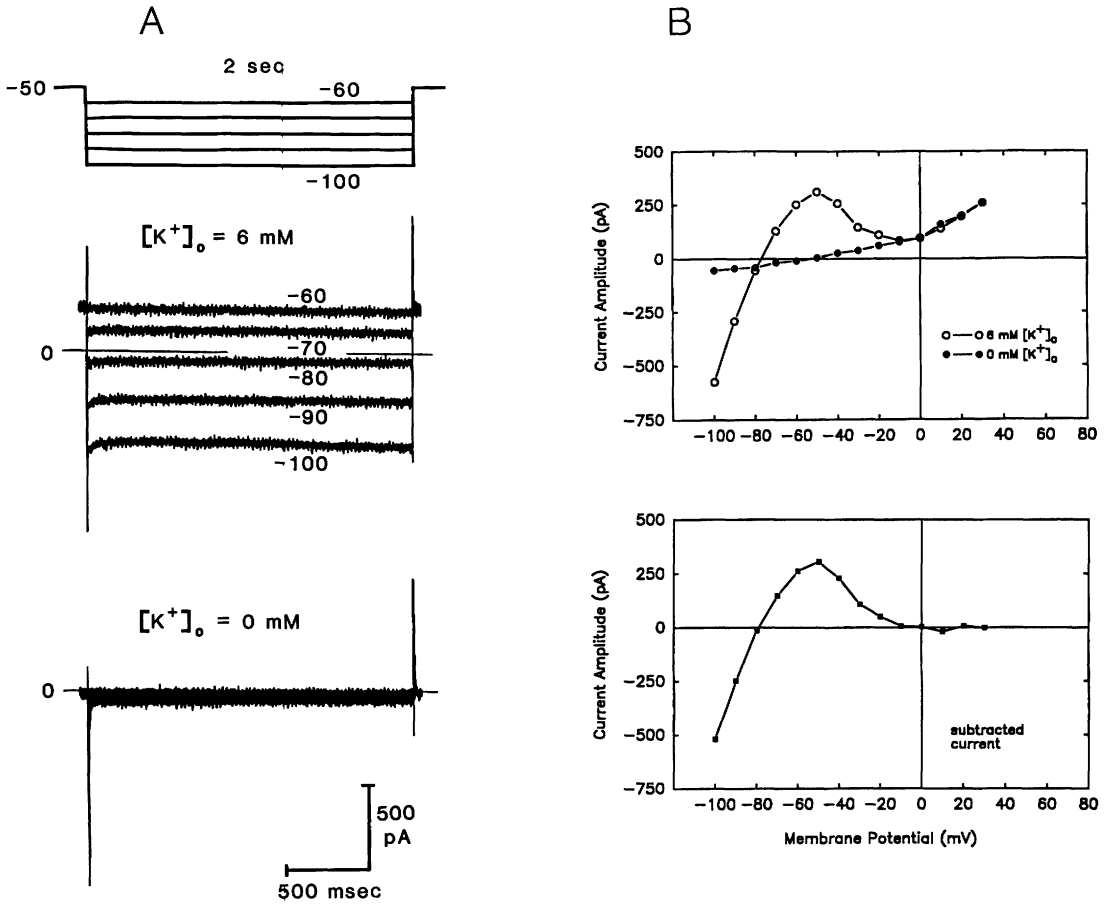

FIGURE 6. *Inward rectifier K^+ current (I_{K1}) measured in a cell from the midmyocardial region using a voltage-step protocol (whole-cell patch-clamp technique). Panel A: Representative tracings of currents elicited by voltage steps from a holding potential of −50 mV to test potentials of −60 to −100 mV in the presence of 6 mM $[K^+]_o$ (middle tracings) and absence of K^+ in the extracellular solution (bottom tracing). The top tracing shows the voltage protocol. Panel B: Current–voltage relations constructed by plotting the current level measured at the end of a 2-second pulse as a function of the test voltage (from −100 to +30 mV, 10-mV steps) in the presence and absence of $[K^+]_o$ (top graph). The bottom graph shows the current–voltage relation obtained by subtraction of the current–voltage relations obtained in the presence and absence of $[K^+]_o$. The bathing solution contained 15 μM tetrodotoxin, 2 mM $MnCl_2$, and 3 μM ouabain throughout the experiment.*

study, we used standard microelectrode, single microelectrode switch voltage-clamp, and whole-cell patch-clamp techniques to examine the characteristics of transmembrane activity and ionic currents in myocytes enzymatically dissociated from discrete layers of the free wall of the canine left ventricle.

Initial characterization of the myocytes was performed using standard microelectrode techniques so as to minimize any alteration of the intracellular milieu. Action potential characteristics and APD–rate relations of myocytes isolated from the epicardial, endocardial, and M regions were remarkably similar to those observed previously in syncytial preparations (Figures 1–4).[1–4,9,21] In another experimental series, we evaluated action potential characteristics in tandem with ionic currents using whole-cell patch recording techniques. Although APD–rate relations were sometimes difficult to quantitate in epicardial and M cells because of loss of the action potential dome at slow frequencies (due to all-or-none repolarization at the end of phase 1), action potential characteristics under these conditions appeared qualitatively similar to those observed using standard microelectrode techniques as well as those previously described in tissues isolated from the respective regions of the heart.

A prominent spike and dome morphology of the action potential was observed with standard microelectrode and patch-pipette recording techniques in myocytes of M region and epicardial origin but not in cells isolated from endocardium. This distinction between epicardium and endocardium was first described and characterized in canine ventricular tissues in vitro.[4] More recently, it has been described in the canine heart[5,6] in vivo, in human ventricular epicardium[24] studied in vitro, and in rabbit[7] and feline[8] ventricular myocytes. The spike and dome configuration appears most prominent in canine and human epicardium, is less so in cat and rabbit epicardium, and is totally lacking in calf epicardium.[1]

These results strongly suggest that the electrophysiological distinctions between epicardium and endocardium are due to differences in the intrinsic electrical properties of the cells and not to electrotonic interactions or differences in the accumulation or depletion of ions in the extracellular space of these tissues.

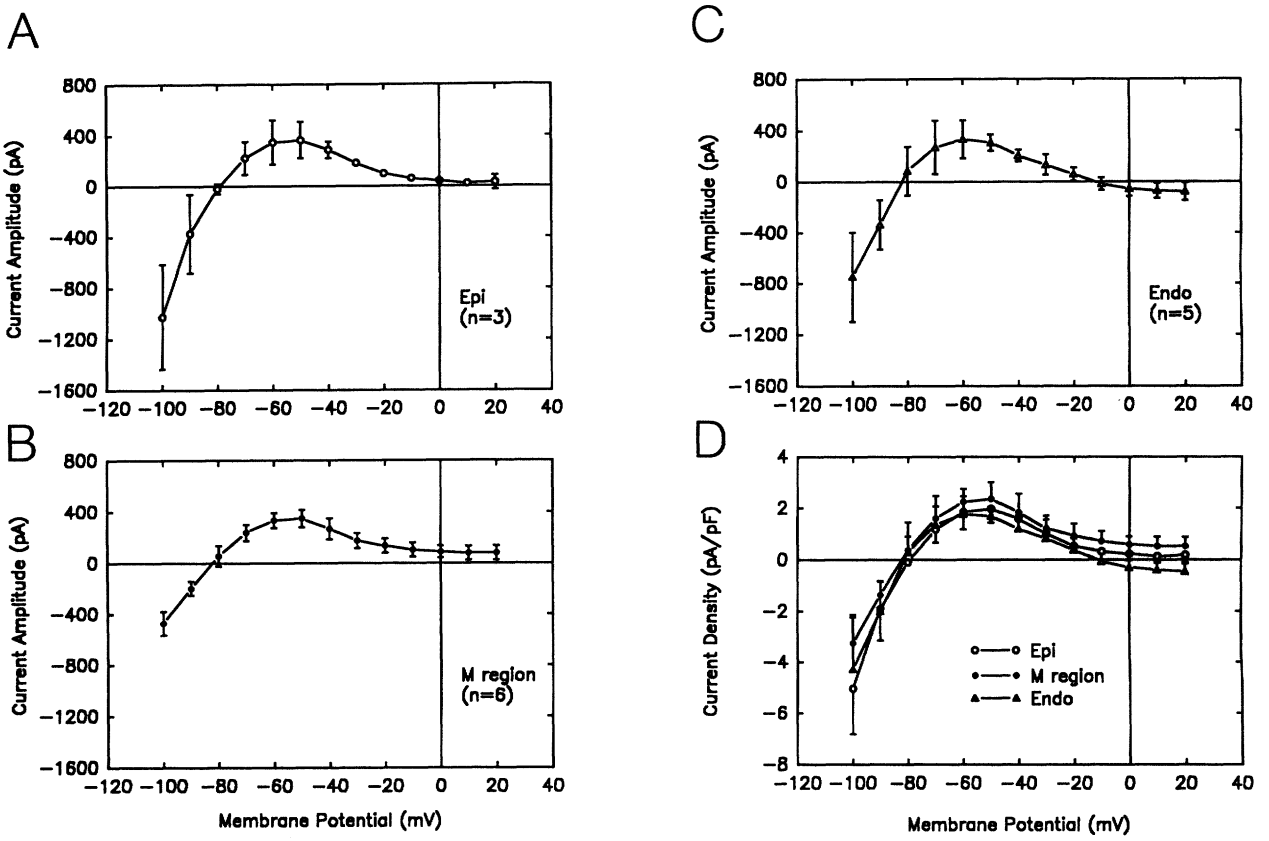

FIGURE 7. *Graphs showing current–voltage relations for the inward rectifier K^+ current (I_{K1}) in myocytes of epicardial (Epi), endocardial (Endo), and midmyocardial (M region) origin. Current–voltage relations (panels A–C) and the current density–voltage relations (panel D) for I_{K1} were determined as illustrated in Figure 6. No significant differences were detected among the three different cell types.*

Our data also provide further evidence in support of the existence of a distinct and unique subpopulation of cells in the deep subepicardial to midmyocardial layers of the canine ventricle. These cells, termed M cells, display characteristics common to both myocardial (spike and dome morphology, absence of phase 4 depolarization) and specialized (higher maximal rate of rise of the action potential upstroke, steeper APD–rate relation) conducting cells. Unlike specialized conducting cells, however, they show no phase 4 depolarization, not even in the presence of catecholamines and low $[K^+]_o$. Action potentials from most myocytes isolated from the M region show a prominent prolongation of APD at slower stimulation rates (steep APD–rate relation).

Cells with prolonged APDs have previously been reported to exist in the deep myocardial layers of transmural preparations obtained in the region of the papillary muscles (canine right and left ventricles).[25] Action potentials with unusually prolonged APDs at slow rates have also been described in single myocytes dissociated from transmural preparations of canine,[13] rat,[26] and guinea pig[27] ventricles. Most recently, Wang et al[28] provided in vivo evidence for the existence of M cells in intact dogs using intramyocardial monophasic action potential recording techniques.

Recent studies designed to assess the distribution of M cells across the canine ventricular wall by mapping transmural slices of the wall indicate that M cells are indeed widely distributed within the ventricular wall and that transitional behavior is apparent throughout, but particularly between midmyocardium and endocardium.[29] In line with this observation, we found a wide range of transitional behaviors in myocytes isolated from the ventricular wall. Figure 15 illustrates superimposed action potentials recorded from six different myocytes at BCLs ranging from 300 to 8,000 msec. Cells 1 and 6 were isolated from epicardial and endocardial regions, respectively. Cells 2–5 were isolated from the M region. They are arranged such that action potentials with the greatest spike and dome are closer to the top (epicardium) and those with a lesser spike and dome are below. The transitional type behavior displayed in cells 2 and 5 was often seen in the myocytes isolated from the interior of the ventricular wall (2–7 mm from the epicardial surface). These findings suggest that the transitional behavior observed in tissues may be due to differences in the intrinsic electrical properties of the cells as well as to electrotonic interactions among the different cell types. In future experiments we plan to isolate and study cells from several discrete levels within the same localized segment of the ventricular wall so as to be able to more precisely correlate the electrophysiological characteristics of the cells with their anatomic site of origin.

Ionic Currents (I_{K1} and I_{to})

Using the switched-clamp technique and KCl-filled microelectrodes to minimize alterations of intracellular

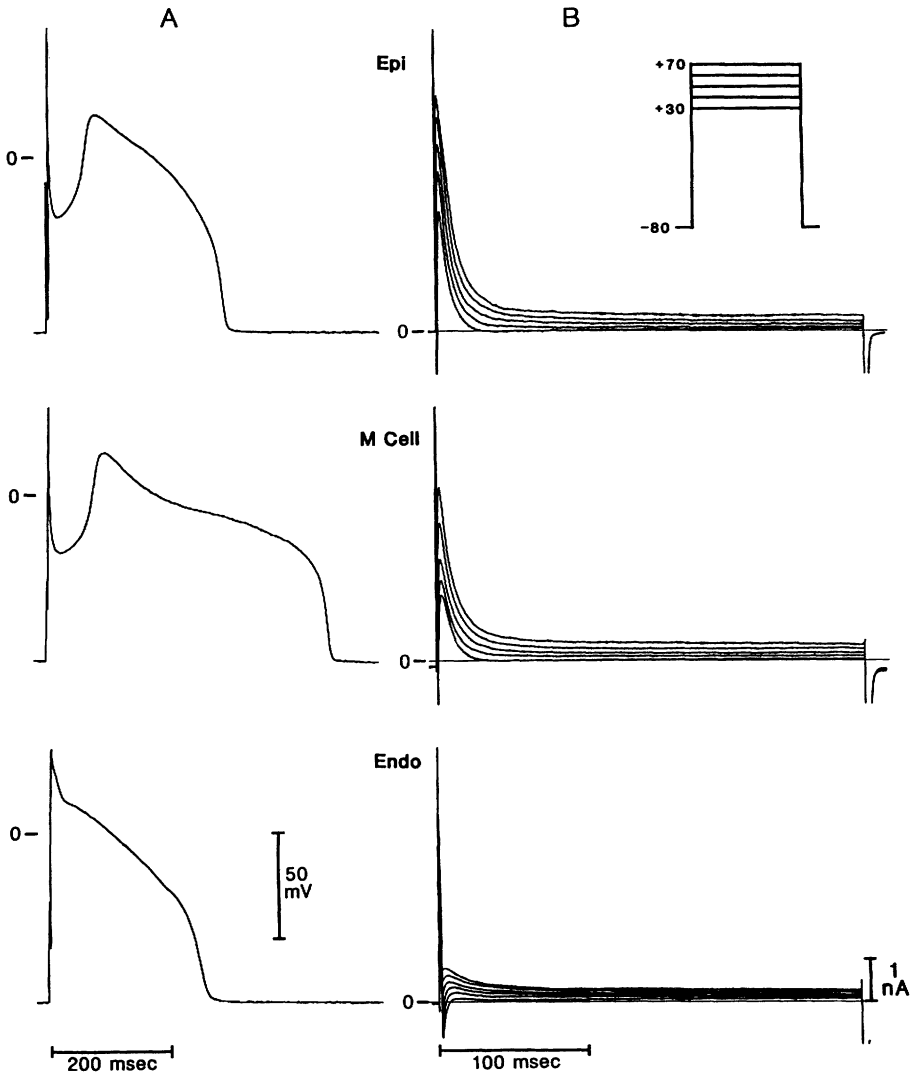

FIGURE 8. *4-Aminopyridine–sensitive transient outward current (I_{to1}) recorded from myocytes of epicardial (Epi), myocardial (M cell), and endocardial (Endo) origin using whole-cell patch-clamp technique. Panel A: Action potentials recorded using patch pipette. Basic cycle length was 2,000 msec. Panel B: Currents recorded from the same cells during 300-msec voltage-clamp steps from a holding potential of −80 mV to test potentials ranging from +30 to +70 mV (10-mV increments). Interval between test pulses was 5 seconds. I_{to1} is most prominent in the Epi myocyte, somewhat less prominent in the M cell, and smallest in the Endo cell. No inward current blockers were used.*

milieu, we initially compared the steady-state I-V relations of the three classes of myocytes. Myocytes from all three regions displayed a similar I-V configuration, with regions of inward rectification, negative slope, and outward rectification (Figure 4). We found no apparent differences in steady-state I-V relations in cells from the three regions. Step and ramp depolarizations elicited under whole-cell patch-clamp conditions also yielded similar steady-state I-V relations in the three cell types. The magnitude of I_{K1} (defined as membrane current blocked by 10 mM CsCl) was comparable in all cell types, averaging 342±97.8 pA (n=21). Similar results were obtained when I_{K1} was defined as the steady-state difference current recorded in the presence and absence of extracellular K^+. The average peak value for I_{K1} using this method was 334±110 pA. These values are larger than those reported for patch-clamped Purkinje myocytes[30] but comparable to values reported in rabbit ventricular myocytes.[31]

It is noteworthy that Furukawa et al[32] recently reported major differences in the characteristics of I_{K1} between epicardial and endocardial myocytes enzymatically dissociated from the cat left ventricle. The steady-state current in these endocardial cells displayed a distinct N-shaped I-V relation; the outward current region was much smaller in the epicardial cells, yielding a blunted N-shaped appearance. The K^+-sensitive component representing I_{K1} was prominent in endocardial but not epicardial cells. This suggests the possibility that important species differences exist between canine and feline ventricular epicardium.

Previous studies from our laboratory suggested that the presence of a prominent I_{to} in canine ventricular epicardium but not endocardium is, in large part, the basis for the prominent spike and dome morphology seen in epicardium but lacking in endocardium.[1,4] We tested this hypothesis by measuring I_{to} in the different cell types. In most experiments, contamination of this current by inward I_{Na} and I_{Ca} was minimized by addition of TTX and Mn^{2+} to the superfusate. Use of 10 mM EGTA in the pipette solution also eliminated the Ca^{2+}-activated component of I_{to} (I_{to2}) and/or Ca^{2+}-activated chloride current.[33] The remaining current, largely abolished by 4-AP, is generally referred to as I_{to1}.

In support of the hypothesis, I_{to1} was found to be very prominent in epicardial cells and much less prominent in endocardial cells (Figures 8–11). In epicardial myocytes, mean amplitude of I_{to1} was 4,203 pA at a test

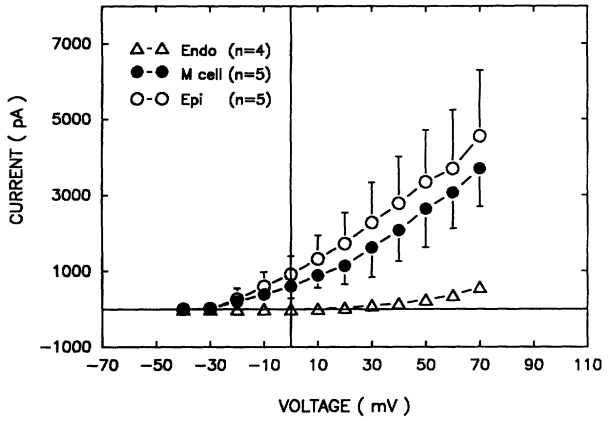

FIGURE 9. *Graph showing average peak current–voltage relations for 4-aminopyridine–sensitive transient outward current (I_{to1}) recorded using the protocol described in Figure 8. Endo, endocardial cells; M cell, cells isolated from deep subepicardial to midmyocardial region; Epi, epicardial cells. No inward current blockers were used. All Epi and M cell measurements of I_{to1} positive to a test potential of +10 mV were significantly different from the current levels measured in Endo cells. Peak I_{to1} in Epi and M cells were not statistically significant from each other at any potential. Values are mean±SD.*

potential of +70 mV. The average value for epicardial cell capacitance was 150±34 pF (Table 1). The calculated I_{to1} density is therefore 28 pA/pF (Table 2). This value is several times that reported in the cat[12] (10 pA/pF; test potential, +80 mV) or rabbit[7] epicardium (15 pA/pF; test potential, +60; 35°C). Our calculated density for I_{to1} in canine endocardial myocytes was 4.9 pA/pF, approximately 1/5 of that recorded in epicardial cells. In rabbit ventricle, Fedida and Giles[7] reported an approximately 50% lower I_{to1} density in papillary muscle cells than in epicardial cells, with endocardial trabecular cells displaying intermediate levels. Furukawa et al[12] observed similar distinctions in I_{to1} between epicardial and endocardial cells isolated from the left ventricle of cat hearts. I_{to1} density was reported to be 10.2±4.8 pA/pF in epicardial myocytes and absent or very small in endocardial myocytes.

The greater amplitude of I_{to1} measured in epicardial versus endocardial myocytes cannot be explained by differences in the voltage dependence of either activation (Figure 11) or inactivation (Figure 12) of the current. The mean $V_{0.5}$ was similar for the three cell types, averaging −40 mV. This value is close to that (−38 mV) reported by Lue and Boyden[34] in canine epicardial myocytes. Values for $V_{0.5}$ of I_{to1} inactivation vary in the literature, with values of −13.5 mV reported for ferret right ventricular myocytes,[35] −23 mV for adult human atrial cells,[36] −38 mV for rabbit ventricular

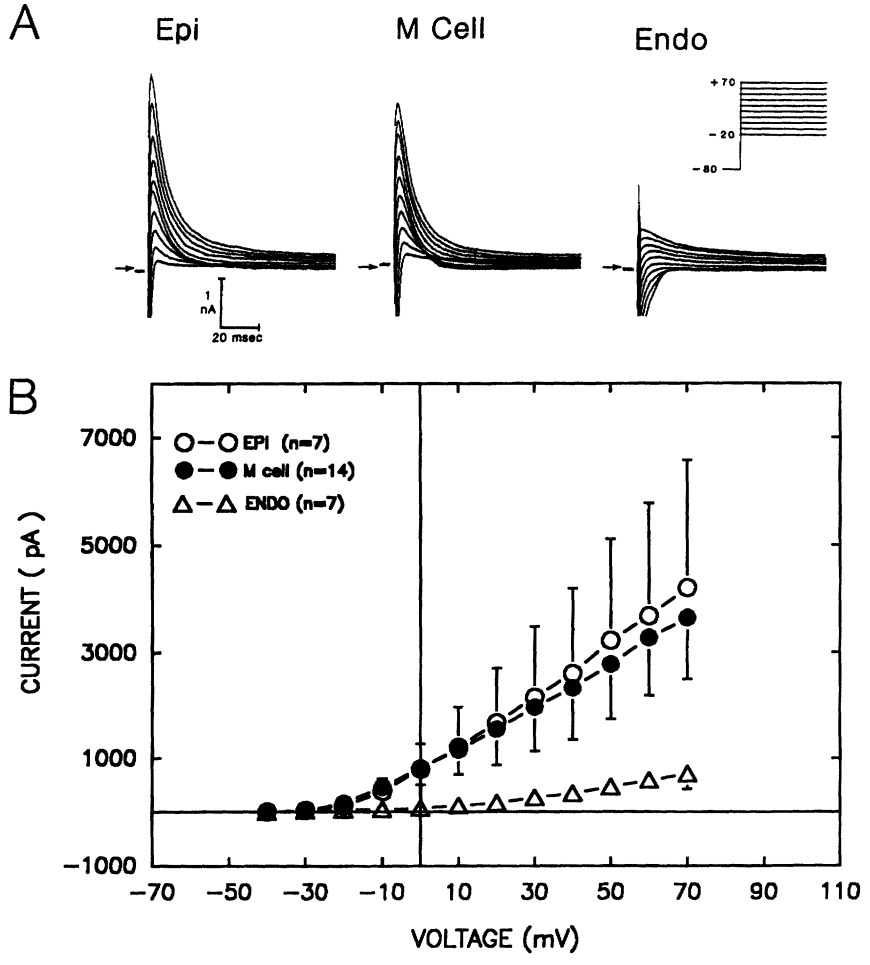

FIGURE 10. *Voltage-dependent activation of the transient outward current (I_{to1}). Panel A: Superimposed current tracings recorded during depolarizing steps from a holding potential of −80 mV to test potentials ranging between −20 and +70 mV (10-mV steps, 300-msec duration) in myocytes of epicardial (Epi), deep subepicardial (M cell), and endocardial (Endo) origin. Initial 100 msec of test pulse is shown. Zero current level is indicated by arrow. External solution contained 15–30 μM tetrodotoxin and 2 mM $MnCl_2$. Panel B: Graph showing average peak current–voltage relation for I_{to1} for each of the three cell types. All Epi and M cell I_{to1} measurements positive to a test potential of 0 mV were significantly different from the current levels recorded in Endo cells. Peak I_{to1} values in Epi and M cells were not statistically significant from each other at any potential. Values are mean±SD.*

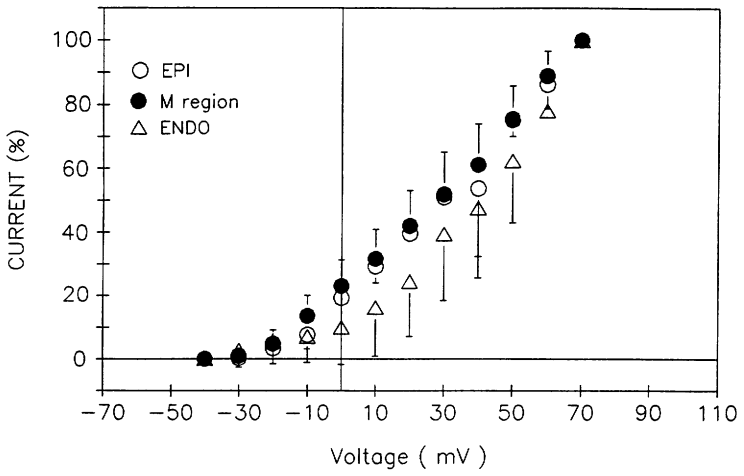

FIGURE 11. *Graph showing normalized peak current–voltage relations for the 4-aminopyridine–sensitive transient outward current (I_{to1}) in myocytes of epicardial (EPI), midmyocardial (M region), and endocardial (ENDO) origin. Amplitudes of peak I_{to1} from Figure 10B are normalized to values obtained at test potentials of +70 mV. Values represent mean±SD. Tetrodotoxin (15–30 μM) and $MnCl_2$ (2 mM) were present throughout. No statistically significant differences were detected at any potential. Values are mean±SD.*

cells,[7] and −57 mV for rat ventricular myocytes.[37] A number of factors, in addition to species differences, can contribute to variability in the quantitation of this parameter: 1) Divalent cations (Co^{2+}, Cd^{2+}, and Ni^{2+}) commonly used as Ca^{2+} channel blockers in the above studies have recently been shown by Agus et al[38] to shift the voltage dependence of I_{to1} activation and inactivation to more positive potentials in rat ventricular myocytes; Mayer and Sugiyama[39] have demonstrated a similar effect of Mn^{2+} in neurons. 2) The 1,4-dihydropyridine Ca^{2+} antagonists and D600 have also been reported to inhibit Ca^{2+}-independent I_{to} in rabbit atrial[40] and rat ventricular[41] myocytes. 3) A recent report by Dukes and Morad[37] also shows modulation of the gating parameters of I_{to1} in rat ventricular myocytes by extracellular but not intracellular Na^+ and Ca^{2+} as well as by TTX. TTX was shown to shift the voltage dependence of inactivation of I_{to1} to more negative potentials[37] in rat ventricular myocytes. Little if any effect of TTX has been noted in other studies involving rat ventricular myocytes.[42]

Currently unknown are the effects of Mn^{2+} on I_{to1} in rat ventricular myocytes or the effects of any of the cations or of TTX on I_{to1} in canine ventricular myocytes. Therefore, we are unable to comment on whether the blockers used in this study influenced $V_{0.5}$. More pertinent to the objective of the present study, however, is the observation that under similar experimental conditions the voltage dependence of inactivation is similar in the three cell types.

Differences in reactivation kinetics, likewise, cannot explain the greater amplitude of I_{to1} in epicardial versus endocardial cells (Figure 14). At −80 mV, recovery from inactivation was found to follow a biexponential time course in most cells. The time constants of the fast and slow components of reactivation averaged 42±23 and 343±206 msec, respectively, when data from all cells were grouped. The time constants recorded in epicardial cells were similar to those of endocardial cells. Cells from the M region, however, displayed longer time constants for both slow and fast components of reactivation, averaging 57±35 and 456±212 msec, respectively. In comparison, Tseng and Hoffman[16] reported time constants of 95 and 610 msec for the two components at −80 mV in myocytes of transmural origin (see Figure 6 of Reference 16). These values are similar to those observed in some of our M cells in the present study (Figure 14) as well as in M cells studied in syncytium using the delta phase 1 restitution method (see Figure 8C of Reference 9). Long time constants have been reported in Purkinje myocytes, although at lower temperature and more positive voltages (fast component, 95 msec; slow component, 922 msec; 20°C; −42 mV). Faster time constants on the order of 25 msec have been reported for rat ventricular cells.[43]

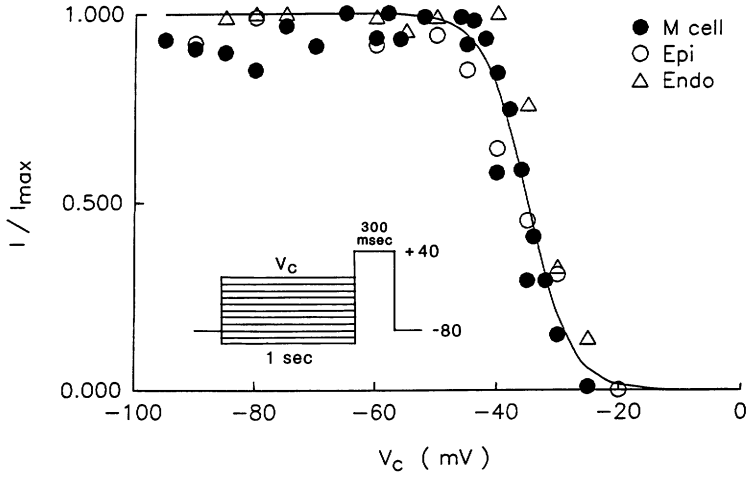

FIGURE 12. *Graph showing voltage dependence of inactivation of the 4-aminopyridine–sensitive transient outward current (I_{to1}) in myocytes of epicardial (Epi), myocardial (M cell), and endocardial (Endo) origin. From a holding potential of −80 mV, cells were depolarized to various conditioning potentials (V_c) for 1,000 msec. The conditioning pulse was followed by a standard test pulse to +40 mV. As the V_c was made more positive, the amplitude of I_{to1} decreased in a sigmoidal fashion. The data are normalized to the largest peak I_{to1} value obtained in each cell (I_{max}). The curve was fit to a Boltzmann distribution as described in the text. The voltage at half-maximal inactivation was −34.9 mV, and the slope factor was 3.6. The external solution contained 30 μM tetrodotoxin and 2 mM $MnCl_2$.*

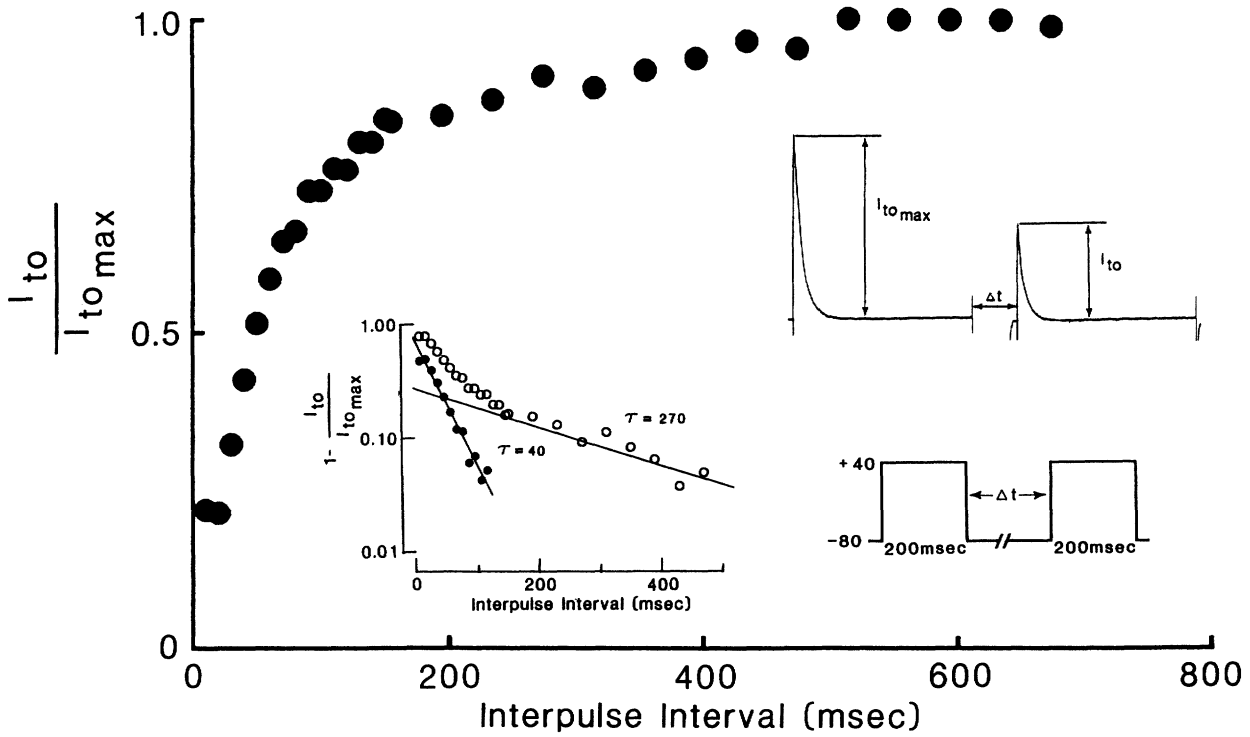

FIGURE 13. *The time course of reactivation of the transient outward current (I_{to}) measured in a cell from the midmyocardial region using a double-pulse protocol (inset). $I_{to_{max}}$, I_{to} amplitude measured during the first pulse. Twin voltage pulses (from −80 to +40 mV, 200-msec duration) were introduced with varying interpulse intervals (Δt) once every 10 seconds. The recovery of I_{to} is plotted as a function of the interpulse interval. Recovery of I_{to} was found to follow a biexponential time course. The two exponential components in this example displayed time constants (τ) of 40 and 270 msec. Time constants were determined as illustrated in the lower left inset (line fit by eye). External solution contained 15 μM tetrodotoxin and 2 mM $MnCl_2$.*

Although the mechanism(s) responsible for the regional differences in I_{to} requires further study, our data point to differences in channel density and/or unitary conductance as the basis for the marked regional differences in I_{to1}. Consistent with this hypothesis are the results of Fedida and Giles.[7] These authors recently reported that single-channel amplitudes, burst open probabilities, and ensemble averages are very similar in rabbit ventricular myocytes from epicardium, endocardial trabeculae, and papillary muscle. Regional differences in I_{to1} among these cell types were concluded to be due to differences in channel density, with epicardial cells showing nearly twice the density of papillary muscle cells.

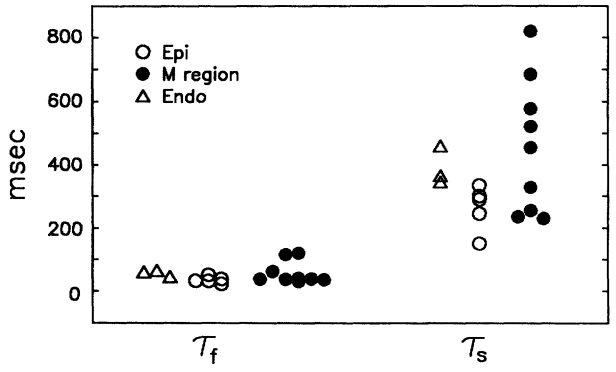

FIGURE 14. *Graph showing time constants of fast (τ_f) and slow (τ_s) components of reactivation of 4-aminopyridine–sensitive transient outward current in myocytes isolated from epicardium (Epi), midmyocardium (M region), and endocardium (Endo). Data points represent the results of individual experiments similar to those illustrated in Figure 13. See text for further discussion.*

Contribution of Other Ionic Currents to Regional Heterogeneity

Differences in ionic currents other than I_{to} undoubtedly contribute to the regional differences in action potential characteristics observed in the canine ventricle. Recent studies using feline myocytes indicate several important differences in the ionic currents that underlie the activity of ventricular epicardium and endocardium. Furukawa et al[44] showed that, compared with endocardial myocytes, ATP-regulated K^+ channels in feline epicardial cells are activated by smaller reductions in intracellular ATP. This group of investigators also reported comparable levels of inward I_{Ca}[45] but a greater density of I_K in epicardial versus endocardial myocytes enzymatically dissociated from the cat left ventricle. Preliminary data from our laboratory point to no significant difference in I_K density between epicardial and endocardial myocytes of the canine left ventricle but to much lower levels of this current in myocytes isolated from the M region of the same hearts (D.-W. Liu and C. Antzelevitch, unpublished observation). A great deal of work clearly remains to be done in defining the distinctions in ionic currents that contribute to regional differences in electrical function.

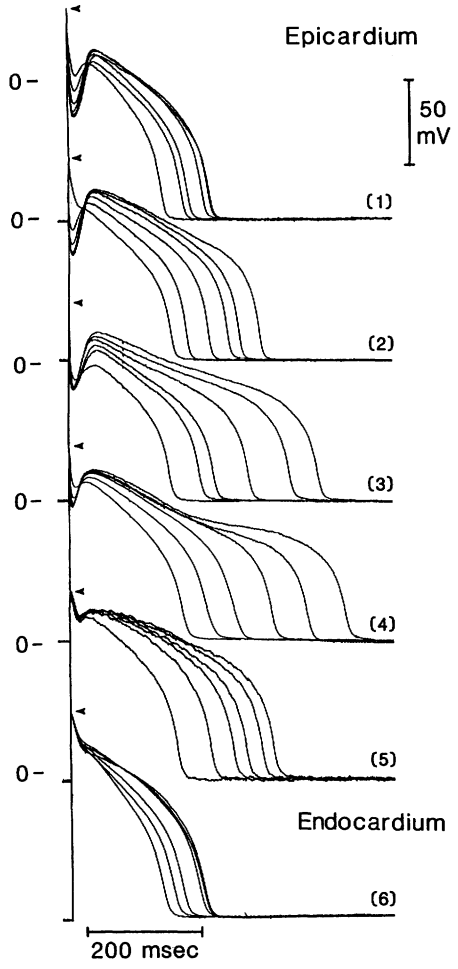

FIGURE 15. *Transmembrane action potentials recorded using standard microelectrodes from six different myocytes disaggregated from epicardial, midmyocardial, and endocardial preparations of the canine left ventricle. Basic cycle lengths were varied over a range of 300–8,000 msec. Cells 1 and 6 were isolated from epicardial and endocardial tissues, respectively. Cells 2–5 were isolated from the midmyocardial region. They are arranged such that action potentials with the greatest spike and dome are closer to the top and those with a lesser spike and dome are below. The transitional type behavior displayed in cells 2 and 5 was often seen in the myocytes isolated from the midmyocardial region. They are also observed in the midmyocardial region of a transmural tissue slice.*

Physiological Implications

Our results provide further support for the existence of marked electrophysiological heterogeneities among cells spanning the ventricular wall of the canine heart. The identification of cells with diverse action potential morphologies and electrophysiological characteristics at different levels of the ventricular wall may contribute to our understanding of a number of basic electrophysiological and electrocardiographic phenomena.

The presence of a prominent I_{to} with slow reactivation kinetics gives rise to a phase of "excess overshoot" in canine ventricular epicardium (Figure 3). During this period, the amplitudes of phases 0 and 1 of the action potentials of early premature beats are larger than those of responses elicited later in diastole.[4] Because of this uncommon restitution characteristic, it is possible for premature beats to conduct under conditions in which basic beats are blocked (supernormal conduction).[1,21] Successful conduction of the premature beats is due to the greater amplitudes of the early phases of the epicardial action potential, which provide for a greater source current in early versus late diastole. M cells share this characteristic of epicardium (Figure 2B) and thus may contribute to the manifestation of a supernormal phase of conduction in ventricular myocardium.[9]

The presence of a prominent I_{to} in epicardium but not endocardium also contributes to differences in the time and rate dependence of APD and refractoriness in these two types of tissue[3] and to a differential sensitivity of these two tissues to depression during exposure to ischemia.[1,46]

The presence of M cells displaying accentuated APD–rate relations in the deep subepicardial to midmyocardial regions of the ventricular wall has several implications. The development of a progressively more prominent dispersion of repolarization and refractoriness within the ventricular wall as stimulation rate is slowed is one consequence. A deep subepicardial or midmyocardial "wall" of refractoriness or "arc of block" would be expected to develop at slow rates, setting the stage for a variety of reentrant arrhythmias, intramural reentry in particular. Intramural reentry has recently been identified as the principal mechanism underlying the initiation and maintenance of ventricular tachycardia leading to ventricular fibrillation during ischemia.[47–50] Bradycardia-induced intramural reentry is well described in the acute stages of ischemia.[51,52]

M cells in the deep subepicardium may also contribute to a number of electrocardiographic manifestations, including long QT intervals, U waves, and drug-induced torsade de pointes. Electrocardiographic U waves and long QT intervals are generally seen at slow rates, and their manifestation is usually enhanced by drugs known to prolong APD and/or induce early afterdepolarizations in the specialized conduction system of the ventricle. A number of hypotheses have been advanced to explain these electrocardiographic phenomena. Prominent among these is the hypothesis that U waves and long QT intervals are due to late repolarization of the Purkinje system and/or the development of early or delayed afterdepolarizations in the Purkinje system. The conduction system, however, has long been argued to be of insufficient mass to generate a distinct U wave on a surface electrocardiogram. We have proposed that M cells, with or without a contribution from the conduction system, are responsible for the manifestation of U waves and long QT intervals in the electrocardiogram.[53]

The presence of a prominent notch or spike and dome morphology in epicardial and M cell action potentials but not in endocardial cells may also contribute to the manifestation of a J wave or Osborne wave in the electrocardiogram.[1,21]

Although beyond the scope of this study, the pharmacology of the M cells is of great interest. Preliminary studies indicate that tissues and cells from the M region, but not those from adjacent epicardial or endocardial regions, develop prominent early and delayed afterdepolarizations and triggered activity in response to a

TABLE 2. Calculated and Measured Densities of the 4-Aminopyridine–Sensitive Transient Outward Current in Myocytes of Epicardial, Midmyocardial, and Endocardial Origin

	Region		
	Epicardium	Midmyocardium	Endocardium
Current amplitudes (pA)			
Mean±SD	4,203±2,370	3,638±1,135	714±286*
n	7	14	7
Capacitance (pF)			
Mean±SD	150±34	142±27	145±44
n	19	30	16
Calculated density (pA/pF)	28.0	25.6	4.93
Measured density (pA/pF)			
Mean±SD	29.0±13.7	32.8±11.6	5.59±3.19*
n	4	9	4

n, Number of cells studied.

Current amplitudes were measured at +70 mV. Calculated densities represent the ratio of average current amplitude (Figure 10) and capacity (Table 1) measurements for all cells from a given region of the myocardium. Measured densities are derived from experiments in which current amplitude and capacity measurements were available for the same cell.

*$p<0.01$ endocardium vs. epicardium or midmyocardium.

variety of drugs.[10,11] The development of early afterdepolarizations and marked action potential prolongation in M cells in response to drugs such as quinidine also provides further insight into our understanding of pharmacologically induced long QT intervals and atypical ventriclar tachyarrhythmias like torsade de pointes that develop under bradycardic and hypokalemic conditions in patients undergoing quinidine therapy.[11]

Summary and Conclusions

Our results demonstrate prominent intrinsic electrophysiological distinctions among cells spanning the ventricular wall of the canine ventricle. Myocytes isolated from the epicardial surface display a prominent spike and dome but a fairly flat APD–rate relation. M cells from the deep subepicardium to midmyocardium exhibit a prominent spike and dome as well as a steep APD–rate relation. Finally, myocytes isolated from the endocardial surface display neither a spike and dome nor a steep APD–rate relation. Transitional behavior is observed as well. These distinctions among myocytes isolated from discrete regions of the ventricular wall are very similar to those observed in syncytial tissues isolated from the respective regions of the wall.

The data provide strong support for the hypothesis that differences in the magnitude of the spike and dome configuration of the action potential in the various cell types are due largely to differences in the contribution of I_{to}. The data also show that the 4-AP–sensitive I_{to}, I_{to1}, of canine epicardial myocytes is several times the density recorded in ventricular myocytes of other species (e.g., cat and rabbit). I_{to1} was characterized in all these three cell types with respect to voltage-dependent activation, inactivation, and reactivation, and it was concluded that differences in the voltage dependence or kinetics of these parameters are unlikely responsible for the regional differences. Further studies are needed to test the hypothesis that these regional differences in I_{to1} are due to differences in channel density. Evaluation of the inward rectifier in the three cell types revealed no important differences. Future work, some already in progress, is aimed at delineation of other ionic currents across the canine ventricular wall.

These findings will hopefully advance our understanding of the basic function of the heart as well as our understanding of the electrocardiographic J wave, T wave, U wave, and long QT intervals. These results may also provide new insights into the mechanisms underlying some forms of cardiac arrhythmia.

Acknowledgments

We are grateful to Drs. Serge Sicouri, Arthur Iodice, Jose Di Diego, and Vladislav Nesterenko for their valuable assistance during the course of this study. We also wish to acknowledge the expert technical assistance of Judy Hefferon and Robert Goodrow.

References

1. Antzelevitch C, Sicouri S, Litovsky SH, Lukas A, Krishnan SC, Di Diego JM, Gintant GA, Liu D-W: Heterogeneity within the ventricular wall: Electrophysiology and pharmacology of epicardial, endocardial, and M cells. *Circ Res* 1991;69:1427–1449
2. Litovsky SH, Antzelevitch C: Differences in the electrophysiological response of canine ventricular subendocardium and subepicardium to acetylcholine and isoproterenol: A direct effect of acetylcholine in ventricular myocardium. *Circ Res* 1990;67:615–627
3. Litovsky SH, Antzelevitch C: Rate dependence of action potential duration and refractoriness in canine ventricular endocardium differs from that of epicardium: The role of the transient outward current. *J Am Coll Cardiol* 1989;14:1053–1066
4. Litovsky SH, Antzelevitch C: Transient outward current prominent in canine ventricular epicardium but not endocardium. *Circ Res* 1988;62:116–126
5. Levine JH, Spear JF, Guarnieri T, Weisfeldt ML, DeLangen CDJ, Becker LC, Moore N: Cesium chloride–induced long QT syndrome: Demonstration of afterdepolarizations and triggered activity in vivo. *Circulation* 1985;72:1092–1103
6. Tande PM, Mortensen E, Refsum H: Rate-dependent differences in dog epi- and endocardial monophasic action potential configuration in vivo. *Am J Physiol* 1991;261:H1387–H1391
7. Fedida D, Giles WR: Regional variations in action potentials and transient outward current in myocytes isolated from rabbit left ventricle. *J Physiol* (Lond) 1991;442:191–209
8. Kimura S, Bassett AL, Furukawa T, Cuevas J, Myerburg RJ: Electrophysiological properties and responses to simulated ischemia in cat ventricular myocytes of endocardial and epicardial origin. *Circ Res* 1990;66:469–477

9. Sicouri S, Antzelevitch C: A subpopulation of cells with unique electrophysiological properties in the deep subepicardium of the canine ventricle: The M cell. *Circ Res* 1991;68:1729–1741
10. Sicouri S, Antzelevitch C: Drug-induced early and delayed afterdepolarizations and triggered activity in deep subepicardial cells (M cells) of the canine ventricle. (abstract) *Circulation* 1990; 82(suppl III):III-645
11. Sicouri S, Antzelevitch C: Afterdepolarizations and triggered activity develop in a select population of cells (M cells) in canine ventricular myocardium: The effects of acetylstrophantidin and Bay K 8644. *PACE* 1991;14:1714–1720
12. Furukawa T, Myerburg RJ, Furukawa N, Bassett AL, Sinichi K: Differences in transient outward currents of feline endocardial and epicardial myocytes. *Circ Res* 1990;67:1287–1291
13. Hewett KW, Legato MJ, Danilo P, Robinson RB: Isolated myocytes from adult canine left ventricle: Ca2+ tolerance, electrophysiology, and ultrastructure. *Am J Physiol* 1983;245:H830–H839
14. Barrington PL, Meier CF Jr, Weglicki WB: Abnormal electrical activity induced by free radical generating systems in isolated cardiocytes. *J Mol Cell Cardiol* 1988;20:1163–1178
15. Hamill OP, Marty A, Neher E, Sakmann B, Sigworth FJ: Improved patch clamp techniques for high-resolution current recording from cells and cell-free membrane patches. *Pflugers Arch* 1981;391: 85–100
16. Tseng G-N, Hoffman BF: Two components of transient outward current in canine ventricular myocytes. *Circ Res* 1989;64:633–647
17. Tseng G-N, Boyden PA: Multiple types of Ca^{2+} currents in single canine Purkinje cells. *Circ Res* 1989;65:1735–1750
18. Siegelbaum SA, Tsien RW: Calcium-activated transient outward current in calf cardiac Purkinje fibers. *J Physiol* (Lond) 1980;299: 485–506
19. Fabiato A: Computer programs for calculating total from specified free or free from specified total ionic concentrations in aqueous solutions containing multiple metals and ligands. *Methods Enzymol* 1988;157:378–417
20. Krishnan SC, Antzelevitch C: Sodium channel block produces opposite electrophysiological effects in canine ventricular epicardium and endocardium. *Circ Res* 1991;69:277–291
21. Antzelevitch C, Litovsky SH, Lukas A: Ventricular epicardium vs. endocardium: Electrophysiology and pharmacology, in Zipes D, Jalife J (eds): *Cardiac Electrophysiology, From Cell to Bedside.* New York, WB Saunders, 1990, pp 386–395
22. Litovsky SH, Sicouri S, Antzelevitch C: Electrophysiologic effects of amiodarone on canine ventricular epicardium and endocardium differ. (abstract) *Circulation* 1990;82(suppl III):III-529
23. Litovsky SH, Antzelevitch C: Differences in electrophysiological responses of canine epicardium and endocardium to changes in [K+]o may explain classical ST-T changes. (abstract) *FASEB J* 1988;15:A930
24. Chiamvimonvat N, Wang L, Kieser TM, Maitland A, Duff HJ: Evidence for a transient outward current in human ventricular epicardium. (abstract) *Circulation* 1991;84(suppl II):II-104
25. Solberg LE, Singer DH, Ten Eick RE, Duffin EG Jr: Glass microelectrode studies on intramural papillary muscle cells. *Circ Res* 1974;34:783–797
26. Watanabe T, Dellbridge LM, Bustamante JO, McDonald TF: Heterogeneity of the action potential in isolated rat ventricular myocytes and tissue. *Circ Res* 1983;52:280–290
27. Watanabe T, Rautaharju P, McDonald TF: Ventricular action potential, ventricular extracellular potentials, and the ECG of guinea pig. *Circ Res* 1985;57:362–373
28. Wang Y, Hariman RJ, Gintant GA, Louie EK, Hwang MH, Loeb HS: A method for recording of intramyocardial monophasic action potential in intact dogs: In vivo evidence of M cells. (abstract) *PACE* 1992;15(suppl II):559
29. Sicouri S, Antzelevitch C: Electrophysiological characteristics and transmural distribution of M cells in the canine ventricle. (abstract) *Circulation* 1991;84(suppl II):II-179
30. Shah AK, Cohen IS, Datyner NB: Background K+ current in isolated canine cardiac Purkinje myocytes. *Biophys J* 1987;52: 519–525
31. Giles WR, Imaizumi Y: Comparison of potassium currents in rabbit atrial and ventricular cells. *J Physiol* (Lond) 1988;405: 123–145
32. Furukawa T, Kimura S, Furukawa N, Bassett AL, Myerburg RJ: Potassium rectifier currents differ in myocytes of endocardial and epicardial origin. *Circ Res* 1992;70:91–103
33. Zygmunt AC, Gibbons WR: Calcium-activated chloride current in rabbit ventricular myocytes. *Circ Res* 1991;68:424–437
34. Lue W, Boyden PA: Abnormal electrical properties of myocardial cells from the chronically infarcted canine heart. *Circulation* 1992; 85:1175–1188
35. Campbell DL, Qu Y, Rasmusson R, Strauss HC: The transient outward potassium current in isolated ferret right ventricular myocytes: A quanititative kinetic analysis. (abstract) *Circulation* 1991; 84(suppl II):II-103
36. Escande D, Coulombe A, Faivre JF, Deroubaix E, Coraboeuf E: Two types of transient outward current in adult human atrial cells. *Am J Physiol* 1987;252:H142–H148
37. Dukes ID, Morad M: The transient K+ current in rat ventricular myocytes: Evaluation of its Ca2+ and Na+ dependence. *J Physiol* (Lond) 1991;435:395–420
38. Agus ZS, Dukes ID, Morad M: Divalent cations modulate the transient outward current in rat ventricular myocytes. *Am J Physiol* 1991;261:C310–C318
39. Mayer ML, Sugiyama K: A modulatory action of divalent cations on transient outward current in cultured rat sensory neurones. *J Physiol* (Lond) 1988;396:417–433
40. Gohto Y, Imaizumi Y, Watanabe M, Shibata RB, Clark RB, Giles WR: Inhibition of transient outward current by DHP Ca2+ antagonists and agonists in rabbit cardiac myocytes. *Am J Physiol* 1991; 260:H1737–H1742
41. Lefevre IA, Coulombe A, Coraboeuf E: The calcium antagonist D600 inhibits calcium-independent transient outward current in isolated rat ventricular myocytes. *J Physiol* (Lond) 1991;432:65–80
42. Kilborn MJ, Fedida D: A study of the developmental changes in outward currents of rat ventricular myocytes. *J Physiol* (Lond) 1990;430:37–60
43. Josephson JR, Sanchez Chapula J, Brown AM: Early outward current in rat single ventricular cells. *Circ Res* 1984;54:157–162
44. Furukawa T, Kimura S, Cuevas J, Furukawa N, Bassett AL, Myerburg RJ: Role of cardiac ATP-regulated potassium channels in differential responses of endocardial and epicardial cells to ischemia. *Circ Res* 1991;68:1693–1702
45. Kimura S, Bassett AL, Furukawa T, Furukawa N, Myerburg RJ: Differences in the effect of metabolic inhibition on action potentials and calcium currents in endocardial and epicardial cells. *Circulation* 1991;84:768–777
46. Lukas A, Antzelevitch C: Does the transient outward current contribute to selective electrical depression of canine epicardium during ischemia? (abstract) *FASEB J* 1988;15:A930
47. Kramer JB, Saffitz JE, Witkowski FX, Corr PB: Intramural reentry as a mechanism of ventricular tachycardia during evolving canine myocardial infarction. *Circ Res* 1985;56:736–754
48. Svenson RH, Littman L, Gallagher JJ, Selle JG, Zimmern SH, Fedor JM, Colavita PG: Termination of ventricular tachycardia with epicardial laser photocoagulation: A clinical comparison with patients undergoing successful endocardial photocoagulation alone. *J Am Coll Cardiol* 1990;15:163–170
49. Pogwizd SM, Corr PB: Mechanisms underlying the development of ventricular fibrillation during early myocardial ischemia. *Circ Res* 1990;66:672–695
50. Janse MJ, Van Capelle FJL, Morsink H, Kleber AG, Wilms-Schopman F, Cardinal R, Naumann D'Alnoncourt C, Durrer D: Flow of "injury" current and patterns of excitation during early ventricular arrhythmias in acute regional myocardial ischemia in isolated porcine and canine hearts: Evidence for two different arrhythmogenic mechanisms. *Circ Res* 1980;47:151–167
51. Scherlag BJ, Kabell G, Harrison L, Lazzara R: Mechanisms of bradycardia-induced ventricular arrhythmias in myocardial ischemia and infarction. *Circulation* 1982;65:1429–1434
52. Patterson E, Scherlag BJ: Pause-dependent facilitation of midmyocardial reentry and phase 1B arrythmia. (abstract) *Circulation* 1989;80(suppl II):II-147
53. Nesterenko VV, Antzelevitch C: Simulation of the electrocardiographic U wave in heterogeneous myocardium: Effect of the local junctional resistance. *IEEE Trans Biomed Eng* (in press)